MyD88 Adaptor-Dependent Microbial Sensing by Regulatory T cells Promotes Mucosal Tolerance and Enforces Commensalism

Sen Wang[1,2], **Louis-Marie Charbonnier**[1,2], **Magali Noval Rivas**[1,2], **Peter Georgiev**[1,2], **Ning Li**[3], **Georg Gerber**[3], **Lynn Bry**[3], and **Talal A Chatila**[1,2]

[1]Division of Immunology, Boston Children's Hospital, Boston, MA 02115, U.S.A

[2]Department of Pediatrics, Harvard Medical School, Boston, MA 02115, U.S.A

[3]Center for Clinical and Translational Metagenomics, Department of Pathology, Brigham & Women's Hospital, Harvard Medical School, Boston, MA 02115, U.S.A.

SUMMARY

Commensal microbiota promote mucosal tolerance in part by engaging regulatory T (Treg) cells via Toll like receptors (TLR). We report that Treg cell-specific deletion of the TLR adaptor MyD88 resulted in deficiency of intestinal Treg cells, a reciprocal increase in T helper-17 (Th17) cells and heightened interleukin-17 (IL-17)-dependent inflammation in experimental colitis. It also precipitated dysbiosis with overgrowth of segmented filamentous bacteria (SFB) and increased microbial loads in deep tissues. The Th17 cell dysregulation and bacterial dysbiosis were linked to impaired anti-microbial intestinal IgA responses, related to defective MyD88 adaptor- and Stat3 transcription factor-dependent T follicular regulatory and helper cell differentiation in the Peyer's patches. These findings establish an essential role for MyD88-dependent microbial sensing by Treg cells in enforcing mucosal tolerance and maintaining commensalism by promoting intestinal Treg cell formation and anti-commensal IgA-responses.
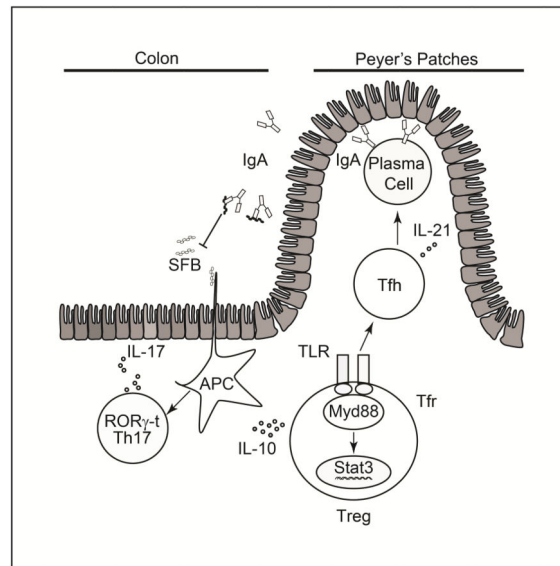
Abstract

SUPPLEMENTAL INFORMATION. Supplemental information includes seven Figures, two Tables, and Supplemental Experimental Procedures and can be found with this article online.

INTRODUCTION

The gastrointestinal commensal microbiota play a critical role in shaping host immune and metabolic responses (Backhed et al., 2005; Chu and Mazmanian, 2013; Lee and Mazmanian, 2010; Round and Mazmanian, 2009). Whereas pathogenic bacteria trigger inflammation and symbiotic bacteria promote tolerance, both sets of responses involve the activation of host pattern recognition receptors (PRR), including toll-like receptors (TLRs) (Hooper et al., 2012; Palm and Medzhitov, 2009). In the case of commensal bacteria, PRR signaling in the absence of tissue damage channels the immune response towards tolerance [reviewed in (Chu and Mazmanian, 2013)]. T regulatory (T_R) cells expressing the transcription factor Foxp3 play a critical role in this process (Josefowicz et al., 2012; Nutsch and Hsieh, 2012; Round and Mazmanian, 2009). How Treg cells sense microbial signals and translate them into a tolerogenic response remains incompletely understood.

Both natural (nTreg) and induced (iTreg) cells contribute to gastrointestinal tolerance (Haribhai et al., 2009; Haribhai et al., 2011). The former are a distinct thymus-derived lineage that express a T cell antigen receptor (TCR) repertoire biased towards self antigens (Hsieh et al., 2004). The latter are induced *de novo* from conventional CD4$^+$Foxp3$^-$ T cells upon encountering antigens in presence of transforming growth factor-β (TGF-β), interleukin-2 (IL-2) and retinoic acid (Coombes et al., 2007; Mucida et al., 2005; Mucida et al., 2007; Sun et al., 2007). iTreg cells carry a distinct TCR repertoire that is biased towards recognition of foreign antigens including the microbiota, reflective of their derivation from conventional T (Tconv) cells (Haribhai et al., 2011; Lathrop et al., 2011; Lathrop et al., 2008). Both nTreg and iTreg cells are required for optimal peripheral tolerance and prevention of intestinal inflammation (Haribhai et al., 2009; Haribhai et al., 2011). In their absence, the microbiota drive intestinal inflammation in a TLR and MyD88-dependent manner (Izcue et al., 2009; Rivas et al., 2012).

Commensal bacteria favor iTreg cell differentiation in the gut (Atarashi et al., 2011; Geuking et al., 2011; Lathrop et al., 2011; Round et al., 2011; Round and Mazmanian, 2010). Promotion by the gut microbiota of Treg cell generation involves TLR signaling, evidenced by the failure to expand colonic lamina propria (cLP) Treg cells in germ free (GF) mice doubly deficient in the TLR adaptor molecules MyD88 and Trif when colonized with altered Schaedler flora (Geuking et al., 2011). TLR2 and TLR4 signaling promotes Treg cell proliferation and survival (Caramalho et al., 2003; Chen et al., 2009; Liu et al., 2006; Sutmuller et al., 2006). Polysaccharide A of *Bacteroides fragilis* signals directly via TLR2 receptors on T cells to promote iTreg cell differentiation and IL-10 and TGF-β production, suppress Th17 cell differentiation and establish colonization of *Bacteroides fragilis* at the mucosal interface (Round et al., 2011; Wang et al., 2006). Collectively, these studies indicate that Treg cells may directly respond to microbial signals, and that this response is important for tolerance acquisition.

To further elucidate the role TLR-MyD88 signaling in Treg cells in promoting mucosal tolerance, we examined the consequences of Treg cell lineage-specific *Myd88* deletion. We identified an essential role for MyD88 in the induction and stability of mucosal Treg cells and the differentiation of T follicular regulatory (Tfr) and helper (Tfh) cells in the Peyer's patches (PP). Furthermore, MyD88 signaling in Treg cells acts via a Stat3-dependent mechanism to promote healthy commensalism by supporting anti-microbial IgA antibody responses, thus suppressing overgrowth of segmented filamentous bacteria (SFB), and restraining Th17 cell responses.

RESULTS

Treg cell-specific MyD88 deletion results in Treg cell deficiency and Th17 cell dysregulation in the gut mucosa

To analyze the role of TLR signaling in Treg cells in maintaining peripheral tolerance, we generated mice with Treg cell-specific MyD88 deficiency by crossing mice harboring a Cre recombinase and an EGFP reporter under the control of the *Foxp3* promoter ($Foxp3^{EGFPcre}$) with others, that carried a floxed *Myd88* allele (Figure S1A) (Hou et al., 2011; Zhou et al., 2009). The resultant mice, termed $Foxp3^{EGFPcre}Myd88^{-/-}$, expressed MyD88 in different tissues examined and in immune cells, including conventional CD4$^+$ T cells, with the exception of CD4$^+$Foxp3$^+$ Treg cells, where transcripts encoding MyD88 were absent in the face of normal expression of *Foxp3* transcripts (Figure S1B). These results indicate that $Foxp3^{EGFPcre}$ was fully effective in specifically deleting *Myd88* in Treg cells while sparing conventional CD4$^+$ T (Tconv) cells. Mice with the *MyD88* lineage-specific deletion were no different in weight and gross phenotype from their MyD88 sufficient littermates (data not shown). The frequency and absolute numbers of Treg cells of MyD88-sufficient ($MyD88^{fl/fl}$) and deficient ($Foxp3^{EGFPCre}MyD88^{-/-}$) littermate mice were similar across most lymphoid tissues, including the thymus, spleen and peripheral lymph nodes. However, the $Foxp3^{EGFPcre}Myd88^{-/-}$ mice exhibited a selective decrease in the Treg cells found in the small and large intestinal lamina propria (sLP and cLP, respectively) as well as those in the PP (Figures 1A and 1B). This decrease was not reproduced by deletion of MyD88-coupled cytokine receptor pathways, including IL-1R1 and IL-18R. It was however recapitulated by

antibiotic-treatment of MyD88-sufficient mice (Figures S1C and S1D). Comparison of MyD88-sufficient and deficient cLP Treg cells revealed that expression of most key Treg cell markers, including Foxp3, CD25, CTLA-4, CD103 and Helios, was not different between the two populations, and that their *in vitro* suppressive capacity was similar (Figures 1C and 1D **and data not shown**). However, expression of Nrp1, associated with nTreg cells, was increased in the cLP of *Foxp3*^{EGFPcre}*Myd88*$^{/}$ mice, suggesting a deficiency in iTreg cells.

To establish the presence of a defect in iTreg cell formation in *Foxp3*^{EGFPcre}*Myd88*$^{/}$ mice, we compared the capacity of naïve CD4$^+$ T cells from *Foxp3*^{EGFPCre} and *Foxp3*^{EGFPcre}*Myd88*$^{/}$ to differentiate into antigen-specific iTreg cells *in vivo*. Naïve CD45.2$^+$CD4$^+$ T cells expressing the OT-II TCR transgene, specific for the OVA$_{323-339}$ peptide in the context of I-A^b, were isolated from either *Foxp3*^{EGFPcre} or *Foxp3*^{EGFPcre}*Myd88*$^{/}$ and transferred into CD45.1$^+$ recipient mice. The latter were subsequently exposed to OVA via the drinking water and examined for the presence of CD45.2$^+$CD4$^+$EGFP$^+$ Treg cells in the cLP. Treg cell-specific MyD88 deficiency resulted in a profound reduction of OVA-induced iTreg cell formation in cLP and mesenteric lymph nodes (MLN), indicating that decreased iTreg cell formation is a key contributor to Treg cell deficiency in intestinal mucosa of *Foxp3*^{EGFPcre}*Myd88*$^{/}$ mice (Figures 1E-G). This deficiency could not be attributed to diminution of intestinal Treg cell proliferation, as revealed by staining with the proliferation marker Ki-67 or by labeling with 5-bromodeoxyuridine (BrdU), nor to increased apoptosis as detected by AnnexinV staining (Figures S1E-G). Also, MyD88-deficient T cells retained the capacity to differentiate to iTreg cells in vitro in response to treatment with anti-CD3 and CD28 mAb and TGF-β (Figure S1H). Analysis of the conserved non-coding sequence 2 (CNS2) at the *Foxp3* locus, whose epigenetic demethylation is necessary for stable Foxp3 expression, revealed decreased CNS2 demethylation in *Foxp3*^{EGFPcre}*Myd88*$^{/}$ Treg cells (Figures 1H and 1I). Together, these results indicate that MyD88 signaling plays a critical role in mucosal iTreg cell induction and epigenetic stability.

Analysis of cLP Treg cells of *Foxp3*^{EGFPcre}*Myd88*$^{/}$ mice uncovered several abnormalities. Flow cytometric and real-time PCR analysis revealed that MyD88-deficient cLP Treg cells exhibited increased expression of the transcription factor RORγ-t (Figures 2A-C)**.** In contrast, expression of the transcription factor GATA-3, implicated in Treg cell stability, was decreased (Figures 2D-F**)** (Wang et al., 2011; Wohlfert et al., 2011). IL-10 expression and *Il10* transcripts were decreased in MyD88-deficient as compared to MyD88-sufficient cLP Treg cells (Figures 2G-I).

In parallel with the contraction of the cLP Treg cell population in *Foxp3*^{EGFPcre}*Myd88*$^{/}$ mice, there was expansion of IL-17-expressing cLP CD4$^+$ Tconv cells (Figures 2J and 2K). The frequency and numbers of cLP CD4$^+$ T cells expressing RORγ-t was also increased (Figures 2L and 2M). In contrast, interferon-γ (IFN-γ) secretion (Figures 2J and 2K) and expression of the T helper-1 (Th1) master regulator T-bet by cLP CD4$^+$ Tconv cells was unchanged (Figure 2N). Similarly, the frequency of IL-22-expressing cLP CD4$^+$ Tconv cells was unchanged, as was the expression of *Il22* transcripts in colonic tissues (data not shown).

Treg cell-specific MyD88 deficiency aggravates the severity of experimental colitis

To determine the functional significance of MyD88 deficiency in Treg cells, we examined the outcome of dextran sodium sulfate (DSS)-induced colitis in $Foxp3^{EGFPcre}Myd88^{-/-}$ mice as compared to control littermate $Myd88^{fl/fl}$ mice. Mice were exposed to DSS at 3.5-5% in drinking water for 5 days then placed on regular water and followed up for another week. Treg cell-specific MyD88 deficiency resulted in aggravated DSS-induced weight loss and mortality associated with increased mucositis as revealed by colon length and histological scoring (Figures 3A-C). This phenotype was rescued by treatment with MyD88-sufficient but not deficient Treg cells, consistent with impaired function of the latter as the underlying mechanism of disease severity. MyD88 deficiency was associated with decreased IL-10 production by Treg cells and increased IL-17 but not IFN-γ production by CD4$^+$ Tconv cells (Figures 3D-I).

To analyze the role of dysregulated IL-17 production in disease severity, we examined the impact of treatment with a neutralizing IL-17 antibody on disease pathogenesis. Results revealed that the anti-IL-17 antibody treatment rescued disease severity in $Foxp3^{EGFPcre}Myd88^{-/-}$ but not $Myd88^{fl/fl}$ control mice (Figures 3J-M). This rescue was associated with decreased frequency and cell number of Th17 but not Th1 cells in $Foxp3^{EGFPcre}Myd88^{-/-}$ (Figure 3M).

Defective function of MyD88-deficient Treg cells in suppressing inflammation was further verified in a second lymphopenia-induced model of colitis. MyD88-deficient Treg cells were ineffective in controlling the colitic response as evidenced by the weight loss, pathological response and dysregulated Th17 and Th1 effector cell responses (Figures S2A-E). Importantly, MyD88-deficient donor Treg cells were prone to lose Foxp3 expression and become pathogenic ex-Treg cells that secreted IFN-γ and IL-17, indicative of increased instability (Figures S2F and S2G).

T$_R$-cell specific MyD88 deficiency impairs intestinal IgA production and increases commensal bacterial translocation to deep tissues

As noted earlier, the defect in mucosal Treg cell populations extended to the PP (Figure 1B). PP Tfr cells have previously been shown to promote luminal IgA production either directly and/or through differentiation into Tfh cells (Cong et al., 2009; Kawamoto et al., 2014; Tsuji et al., 2009). As compared to WT Tfh cells, those of $Foxp3^{EGFPcre}Myd88^{-/-}$ mice were decreased in frequencies and numbers and exhibited decreased expression of the cytokine IL-21, important for B cell germinal center response (Figures 4A and 4B). Tfr cells were more severely compromised (Figures 4C), and they exhibited decreased expression of canonical Tfr cell markers including BCL-6, ICOS, and CD40L (Figures S3A and S3B). In contrast, both cell populations were not altered in the mesenteric lymph nodes (data not shown). We examined $Foxp3^{EGFPcre}Myd88^{-/-}$ and control $Myd88^{fl/fl}$ littermate mice for their frequencies of IgA positive B cells in the PP. Results revealed decreased frequencies of switched IgA$^+$B220$^+$ B cells and IgA$^+$B220$^-$ cells (the latter composed mostly of CD138$^+$ plasma cells) in the PP of $Foxp3^{EGFPcre}Myd88^{-/-}$ mice (Figure 4D **and data not shown**). The intestinal luminal, but not serum, IgA concentrations were decreased also in $Foxp3^{EGFPcre}Myd88^{-/-}$ as compared to $Myd88^{fl/fl}$ mice, and it remained so in the context of

DSS-induced colitis mice (Figure 4E). In contrast, serum and intestinal luminal concentrations of IgG, and of IgG1 and IgG2a subclasses, were similar in the two mouse strains (Figure 4E). Antibiotic treatment of WT mice reproduced the effects of Treg cell-specific MyD88 deficiency in terms of decreased Tfh and Tfr frequencies in the PP and depressed luminal but not serum IgA concentrations, indicating that the adverse effects of MyD88 deficiency on gut IgA responses resulted from the interruption of microbial sensing by Treg cells (Figure S3C-E).

We further investigated the impact of MyD88 Treg cell deficiency on the differentiation of antigen-specific Tfr and Tfh cells in the PP by means of adoptive transfer experiments. First, we examined the capacity of sorted splenic $Foxp3^{EGFPcre}$ and $Foxp3^{EGFPcre}Myd88^{\,/\,}$ Treg cells transferred into $Tcra^{-/-}$ mice to differentiate into Tfr and Tfh cells in the PP and support luminal IgA production. Results showed that whereas the total numbers of T cells in the PP were similar in the two transfer groups (**data not shown**), the frequencies and absolute numbers of $Foxp3^{EGFPcre}Myd88^{\,/\,}$-derived PP Tfh cells were decreased as compared to $Foxp3^{EGFPcre}$-derived cells (Figure 4F). In particular, $Foxp3^{EGFPcre}Myd88^{\,/\,}$ Tfr cells were profoundly decreased both in frequencies and cell numbers as compared to those derived from $Foxp3^{EGFPcre}$ cells (Figure 4G). In contrast, the frequencies and numbers of $Foxp3^{EGFPcre}Myd88^{\,/\,}$ Treg cells in the spleens of recipient mice were similar to those of transferred Foxp3^{EGFPCre} Treg cells (data not shown). The percentage of IgA$^+$B220$^+$ and the concentrations of luminal IgA were all markedly decreased in $Tcra^{-/-}$ mice receiving $Foxp3^{EGFPcre}Myd88^{\,/\,}$ as compared to $Foxp3^{EGFPcre}$ Treg cells. In contrast, luminal IgG1 concentrations were similar between the two groups (Figures 4H and 4I).

To rule out a role for changes in Treg cell TCR repertoire induced by MyD88 deficiency in the observed results, we carried out transfer studies using OT-II$^+$ TCR transgenic cells, specific for OVA$_{323-339}$ peptide. Naïve CD4$^+$Foxp3$^-$ T cells isolated from OT-II$^+$ $Foxp3^{EGFPcre}$ or OT-II$^+$ $Foxp3^{EGFPcre}Myd88^{\,/\,}$ mice were transferred into $Tcra^{-/-}$ mice. The recipients were fed OVA in the drinking water for one week then examined for the differentiation of the donor T cells in the PP into Tfr and Tfh cells. Results revealed that there was no difference in the frequency of donor cells in the spleens of recipient mice (data not shown). In the PP, the frequencies of OT-II$^+$ Tfh and Tfr cells were markedly reduced in $Tcra^{-/-}$ recipients of naïve CD4$^+$ T cells from $Foxp3^{EGFPcre}Myd88^{\,/\,}$ as compared to $Foxp3^{EGFPcre}$ mice (Figures S4A and S4B). The frequencies of PP IgA$^+$B220$^+$ B cells, concentrations of luminal IgA and titers of luminal OVA-specific IgA antibodies were similarly reduced (Figures S4C and S4D). The reduced capacity of naïve OT-II$^+$CD4$^+$ T cells of OT-II$^+$ $Foxp3^{EGFPcre}Myd88^{\,/\,}$ mice to support Tfh and Tfr cell differentiation in PP, luminal IgA production and luminal OVA-specific IgA responses was reproduced when OT-II$^+$ $Foxp3^{EGFPcre}Myd88^{\,/\,}$ Treg cells were isolated and transferred into $Tcra^{-/-}$ (Figures S4E-H). These results indicate that the antigen-driven differentiation of Tfr and Tfh cells in the PP from both naïve CD4$^+$ T cell precursors and preformed Treg cells was dependent on Treg cell-intrinsic MyD88 signaling.

Intestinal IgA production controls pathobionts and maintains commensalism (Cong et al., 2009; Fagarasan et al., 2010; Peterson et al., 2007). Significantly, analysis revealed decreased IgA bound to bacteria in fecal pellets of $Foxp3^{EGFPcre}Myd88^{\,/\,}$ as compared to

Myd88^{fl/fl} mice, indicative of decreased IgA anti-bacterial responses (Figure 5A). The functional implications of luminal IgA deficiency in *Foxp3^{EGFPcre}Myd88^{−/−}* mice were further examined using a non-pathogenic *E. coli* (DH5α strain) that expressed a chicken Ovalbumin (OVA) protein fragment (amino acids 139–386). Oral gavage with OVA-DH5α *E. coli* revealed profoundly decreased luminal OVA-specific IgA, but not IgG1, consistent with impaired bacteria-specific IgA antibody responses (Figure 5B).

To determine whether impaired gut anti-microbial IgA responses were associated with altered small intestinal microbiota communities, we performed direct highly parallel pyrosequencing of 16S ribosomal DNA (rDNA) amplicons derived from illeal tissues of *Foxp3^{EGFPcre}Myd88^{−/−}* and *Myd88^{fl/fl}* mice (see Supplemental Experimental Procedures section for description of the sequencing methods and bioinformatic analysis). Analysis of microbiota diversity using the Shanon measure revealed no differences between *Myd88^{fl/fl}* and *Foxp3^{EGFPcre}Myd88^{−/−}* mice (**data not shown**). However, Unifrac analysis showed significant differences in the microbial community structure between *Myd88^{fl/fl}* and *Foxp3^{EGFPcre}Myd88^{−/−}* mice (Figure 5C). Statistical testing at the level of bacterial phyla revealed increased relative abundance of *Firmicutes* and decreases in *Bacteroidetes* and *Tenericutes* phyla in *Foxp3^{EGFPcre}Myd88^{−/−}* as compared to *Myd88^{fl/fl}* mice (Figure 5D). Analysis of taxa that discriminated between the two groups of mice identified 6 taxa at the genus level, encompassing 16 Operational Taxonomic Units (OTUs) (Tables S1 and S2). The most abundant of the latter, OTU0006, was detected in *Foxp3^{EGFPcre}Myd88^{−/−}* but not *Myd88^{fl/fl}* samples (Figure 5E and Table S1). It was identified by phylogenetic placement and sequence alignment as SFB, consistent with the role of IgA in immunity to SFB (Figure S5) (Gaboriau-Routhiau et al., 2009; Ivanov et al., 2009; Lecuyer et al., 2014; Suzuki et al., 2004). Magnetic cell sorting of IgA-bound fecal bacteria followed by real time PCR analysis revealed that SFB sharply segregated into the IgA^+ fraction in *Myd88^{fl/fl}* mice, in agreement with recent studies (Palm et al., 2014). In contrast, it was increased in both the IgA^+ and IgA^− fractions in *Foxp3^{EGFPcre}Myd88^{−/−}* mice (Figure 5F). These studies suggest that the SFB dysbiosis in *Foxp3^{EGFPcre}Myd88^{−/−}* mice was related to the defective anti-bacterial IgA response.

Dysbiosis in *Foxp3^{EGFPcre}Myd88^{−/−}* mice was associated with increased bacterial translocation into deep tissues. Oral gavage of OVA-DH5α *E. coli* resulted in its increased recovery in the fecal pellets and livers of *Foxp3^{EGFPcre}Myd88^{−/−}* mice as compared to *Myd88^{fl/fl}* controls (Figure 5G). More broadly, the livers and lungs of *Foxp3^{EGFPcre}Myd88^{−/−}* had increased bacterial loads as compared to those of *Myd88^{fl/fl}* mice, with increased recovery of *Lactobacilli* and *Pasteurella* species in both organs (Figure 5H). Overall, these results indicate that MyD88 expression in Treg cells enable optimal intestinal IgA antibody responses to commensal bacteria and protect against dysbiosis and unrestrained gut bacterial translocation to deep tissue.

Rescue with IgA^+ PP B cells restores luminal IgA and corrects the skewed intestinal Th17 cell response

To determine the relationship of the deficient luminal IgA response to the commensal bacteria and the dysregulated intestinal Th17 cell response, we conducted studies in which

IgA$^+$ or IgG1$^+$ B cells derived from the PP of WT CD45.1$^+$ C57BL/6 mice were isolated by cell sorting and transferred into CD45.2$^+$ *Foxp3^{EGFPcre}Myd88$^{/}$* mice (Figure 6A). The recipient mice were examined for luminal IgA concentrations and intestinal Treg and Th17 cell populations. Transfer of IgA$^+$ but not IgG1$^+$ PP B cells corrected the luminal IgA deficiency without impacting the luminal IgG or serum IgA or IgG concentrations (Figure 6B). Importantly, transfer of IgA$^+$ but not IgG$^+$ PP B cells reversed the Th17 cell skewing in the intestinal cLP without impacting Th1 cells, indicating that the increase in LP Th17 cells in *Foxp3^{EGFPcre}Myd88$^{/}$* mice was a consequence of deficient intestinal luminal IgA (Figures 6C and 6D). In contrast, the deficiency in LP Treg and PP Tfr cells was not corrected, indicating an intrinsic function for MyD88 signaling in promoting intestinal Treg cell responses (Figures 6E and 6F).

IgA regulates the abundance of segmented filamentous bacteria (SFB), instigators of Th17 cell differentiation in the gut (Gaboriau-Routhiau et al., 2009; Ivanov et al., 2009; Lecuyer et al., 2014; Suzuki et al., 2004). Real time PCR Analysis of SFB 16S rRNA in the ileal tissues and in the stool revealed their elevation in *Foxp3^{EGFPcre}Myd88$^{/}$* mice as compared to WT controls. Rescue with PP IgA$^+$ but not IgG$^+$ B cells suppressed the increase in SFB rDNA content in the fecal pellets of *Foxp3^{EGFPcre}Myd88$^{/}$* mice (Figure 6G). Transfer of PP IgA$^+$, and to a lesser extent IgG$^+$ B cells also suppressed the translocation of DH5α *E. coli* bacteria into the liver (Figure 6H). Overall, these results indicate that the expansion in Th17 cells in *Foxp3^{EGFPcre}Myd88$^{/}$* mice and the increased bacterial translocation into deep tissues were consequences of the failure luminal IgA immunity in suppressing SFB and commensal invasiveness, respectively.

IL-10 production by Treg cells has been implicated in the regulation of Th17 cell differentiation (Rubtsov et al., 2008). Because MyD88-deficient Treg cells expressed reduced amounts of IL-10 (Figures 2G and 2H), we examined whether IL-10 deficient Treg cells impacted gut IgA production. Transfer studies in *Tcra$^{−/−}$* mice revealed that IL-10 sufficient or deficient Treg cells were equally effective in supporting PP Tfh and Tfr cell differentiation, IgA$^+$B220$^+$ B cell expansion, luminal IgA production and the IgA anti-microbial response (Figures S6A-E). These results indicate that the effects of MyD88 deficiency on PP Tfh and Tfr cell differentiation and gut IgA production are not related to their decreased IL-10 production.

Treg cell specific MyD88 signaling regulates the luminal IgA-SFB-Th17 cell axis by a Stat3-dependent mechanism

To elucidate the mechanism by which MyD88 signaling in Treg cells regulates mucosal tolerance, we examined the activation by TLR signaling of the down-stream transcription factors NF-κB and Stat3. Both transcription factors were phosphorylated in response to a common TLR1-2 ligand in MyD88-sufficient but not - deficient cLP Treg cells (Figures 7A and 7B; Figures 7D and 7E). Chromatin immunoprecipitation assays revealed that both factors bound the *Foxp3* CNS2 following TLR1-2 stimulation of MyD88-sufficient but not deficient cLP Treg cells (Figures 7C and 7F). In contrast, IL-2 stimulation resulted in Stat5 phosphorylation and its translocation to the CNS region in both MyD88-sufficient and deficient cLP Treg cells (Figures 7 G-I). Also, IL-10 treatment induced Stat3

phosphorylation equally well in MyD88-sufficient and deficient Treg cells, indicating that MyD88-related signaling defects were TLR-stimulation specific (Figures S7A and S7B).

TLR-MyD88 signaling classically activates the transcription factor NF-κB (Kawai and Akira, 2007). We therefore examined the capacity of augmented NF-κB activation in Treg cells to rescue IgA deficiency in $Foxp3^{EGFPcre}Myd88^{/}$ mice by using a $Foxp3^{EGFPcre}$-regulated transgene encoding a gain of function Inhibitor of Kappa B kinase Beta mutant ($R26^{IIkbkb}$) (Sasaki et al., 2006). Expression of the $R26^{IIkbkb}$ transgene upregulated the phosphorylation of p65 subunit of NF-κB in Treg cells both at rest and following stimulation with a TLR1-2 ligand (Figures S7C-F). Transgene expression in Treg cells failed to correct the deficit in luminal IgA concentrations in $Foxp3^{EGFPcre}Myd88^{/}$ mice, while leaving those of Foxp3^{EGFPCre} mice unaffected. It also did not affect the luminal total IgG concentrations in both mouse strains (Figure S7G). Significantly, transgene expression decreased PP Tfr and cLP Treg cells and increased the cLP Th17 cells, indicating that it promoted Treg cell conversion in to Th17 cells (Figure S7H, I). Transgene expression did not significantly affect SFB abundance in $Foxp3^{EGFPcre}$ mice, but compounded the SFB expansion in $Foxp3^{EGFPcre}Myd88^{/}$ mice (Figure S7J). Overall, these data indicate that the deficit in IgA production in $Foxp3^{EGFPcre}Myd88^{/}$ mice cannot be rescued by augmented activation of NF-κB in Treg cells.

Stat3 has been implicated in Tfh differentiation (Ma et al., 2012). Treg cell-intrinsic Stat3 signaling also promotes iTreg cell generation and is required for the regulation of Th17 cells (Chaudhry et al., 2009; Laurence et al., 2012). $Foxp3^{EGFPcre}Stat3^{/}$ mice, with Treg cell-specific Stat3 deficiency, recapitulated key phenotypes of $Foxp3^{EGFPcre}MyD88^{/}$ mice. They exhibited reduced PP IgA$^+$, but not IgG$^+$, B cells and decreased intestinal IgA, but not IgG, antibody concentrations. Both deficiencies were rescued by the transfer of PP IgA$^+$ but not IgG$^+$ B cells (Figures 7J and 7K). Similar to $Foxp3^{EGFPcre}Myd88^{/}$ mice, $Foxp3^{EGFPcre}Stat3^{/}$ mice exhibited reduced cLP Treg cells and PP Tfr cells that were not restored by the transfer of either PP IgA$^+$ or IgG$^+$ B cells (Figures 7L and 7M). Importantly, transfer of PP IgA$^+$, but not IgG$^+$ B cells to Foxp3^{EGFPCre}Stat3$^{/}$ mice completely suppressed the dysregulated cLP Th17 cell response previously described in these mice while leaving unaffected the cLP Th1 cell response (Chaudhry et al., 2009) (Figure 7N). The dysregulated cLP Th17 cell response of $Foxp3^{EGFPcre}Stat3^{/}$ mice was associated with overgrowth of SFB, which was also effectively suppressed by the transfer of PP IgA$^+$ but not IgG$^+$ B cells (Figures 7O). Overall, these results implicate Stat3 activation as the critical mechanism by which by MyD88 signaling regulates IgA production, SFB commensalism and Th17 cell responses.

Discussion

Our studies revealed MyD88-dependent microbial sensing by Treg cells as serving to coordinately regulate gut mucosal cellular and humoral adaptive immune responses in favor of tolerance. MyD88 signaling promoted the generation of antigen-specific iTreg cells at the mucosal interface, including LP and PP. Its deficiency in Treg cells impaired the regulation of inflammatory responses in two different models of microbial flora-dependent gut inflammation, including DSS and lymphopenia-induced colitis. A second cardinal function

of MyD88 signaling in Treg cells is its promotion of IgA immunity to the commensal flora by virtue of its regulation of Tfr and Tfr-derived Tfh cell differentiation in the PP. Together, these functions of MyD88 signaling in Treg cells enable the maintenance of healthy commensalism and restrain microbiota-driven dysregulated mucosal immune responses.

T_R-specific MyD88 deficiency compromised the LP and PP Treg cell populations. The mucosal Treg cell deficit reflected impairment of *in vivo* induction of iTreg cells in the face of normal development of nTreg cells in the thymus, consistent with enrichment of gut tissues with microbiota-specific iTreg cells. In contrast, splenic Treg cells, which are predominantly thymus derived, were unaffected. MyD88 deficiency also resulted in Treg cell instability, with increased generation of Foxp3$^-$ ex-Treg cells in the context of mucosal inflammation, such as lymphopenia-induced colitis, and poor epigenetic demethylation of Foxp3 CNS2.

A major finding of our studies is that Treg cell-specific MyD88 signaling regulates the gut commensal flora. Its deficiency altered gut microbial community structure and composition. It resulted in dysbiotic expansion of SFB, a pathobiont that drives Th17 cell differentiation, accounting for the dysregulated expansion of the latter in *Foxp3^{EGFPcre}Myd88$^{/}$* mice. It also promoted commensal bacterial invasiveness, with increased bacterial translocation in to deeper tissues. A key mechanism by which Treg cell-specific MyD88 signaling influences the gut microbiota is through its promotion of anti-commensal IgA responses by virtue of its regulation of Tfh and IgA$^+$ B cell differentiation in the PP. Transfer of IgA$^+$ B cells completely suppressed the SFB expansion and reversed the Th17 cell dysregulation in *Foxp3^{EGFPcre}Myd88$^{/}$* mice, thus linking the failure of IgA immunity with Th17 cell-mediated immune dysregulation. Transfer of IgA$^+$ B cells did not ameliorate the Treg cell deficit in the gut, reflecting a requirement for MyD88 signaling in differentiating Treg cells. Our results support a key role for MyD88 in directing Tfr to Tfh cell differentiation in PP, a differentiation step previously proposed by Fagarasan et al (Kawamoto et al., 2014; Tsuji et al., 2009). Th17 cells have also been proposed to promote serum IgA responses when transferred into *Tcra$^{-/-}$* mice (Hirota et al., 2013). However, serum IgA responses were unchanged in *Foxp3^{EGFPcre}Myd88$^{/}$* mice despite increased mucosal Th17 cells.

Mechanisms by which MyD88 promoted mucosal Treg cell generation and directed luminal IgA responses appeared to involve Stat3, whose activation by TLR may proceed via a MyD88-DOCK8 signaling cascade (Jabara et al., 2012). Consistent with such a mechanism, Stat3 activation in Treg cells treated with TLR ligands was abrogated by MyD88 deficiency. T_R-cell specific Stat3 deficiency, which has been previously shown to precipitate Th17 cell dysregulation, recapitulated the other key phenotypes of T_R-cell specific MyD88 deficiency including decreased mucosal Treg cells, impaired PP IgA$^+$ B cell differentiation and luminal IgA production, and SFB dysbiosis (Chaudhry et al., 2009). In both cases, the IgA deficit, SFB dysbiosis and Th17 cell dysregulation but not the mucosal Treg cell deficiency were reversed by the transfer of PP IgA$^+$ B cells. Whereas Treg cell-specific Stat3 deficiency induces spontaneous age-dependent gut inflammation in affected mice, the phenotype of Treg cell-specific MyD88 deficiency is milder, with its disease promoting function becoming pronounced in the context of an inflammatory stimulus (DSS or lymphopenia-induced colitis) (Chaudhry et al., 2009). This difference may relate to the fact that MyD88

deficiency does not disrupt non-TLR-dependent Stat3 activation in Treg cells, such as that induced by IL-10, which may provide an additional layer of immunoregulation at steady state (Chaudhry et al., 2011).

While NF-κB promotes thymic Treg cell development and is activated by MyD88, Treg cell-specific expression of a gain of function IKK beta kinase mutant failed to rescue the phenotype of IgA efficiency in $Foxp3^{EGFPcre}Myd88^{-/-}$ mice (Long et al., 2009). Instead, it induced decreased mucosal Treg cells and increased Th17 cells in otherwise MyD88 sufficient mice, suggesting that sustained NF-κB activation in mucosal Treg cells, such as in the context of an inflammatory environment, may favor their switching into Th17 cells. Accordingly, it can be postulated that the outcome of MyD88 signaling in promoting iTreg cell differentiation may well depend on a balanced Stat3: NF-κB signaling and the interaction of the respective pathways with Foxp3.

In summary, MyD88 signaling in Treg cells integrates cues from the gut microbiota to augment the mucosal Treg cell compartment and to enforce commensalism by directing anti-microbial IgA responses. It thus provides an unusual example of a Treg cell pathway that promotes, rather than suppresses, immune responses in the service of tolerance induction.

Materials and Methods

Mice

CD45.1⁺, CD45.2⁺OT-II⁺, $Foxp3^{EGFPcre}$, $Foxp3^{EGFP}$, $Myd88^{fl/fl}$, $Stat3^{fl/fl}$, $R26^{IIkbkb}$, $Il18r^{-/-}$, $Il1r1^{-/-}$, $Il10^{-/-}$, $Rag1^{-/-}$ and $Tcra^{-/-}$ mice, all on C57BL6/J background, were obtained from the Jax Lab (Haribhai et al., 2007; Murtaugh et al., 2003; Sasaki et al., 2006; Yang et al., 2004; Zhou et al., 2009). $Myd88^{-/-}$ mice were a gift from S. Akira (Osaka University, Osaka, Japan) and were crossed with $Foxp3^{EGFP}$ mice (Rivas et al., 2012). All mutant mouse strains and their respective crosses were backcrossed 8-10 generations on C57BL/6 background. The mice were housed under specific pathogen-free conditions and used according to the guidelines of the institutional Animal Research Committees at the Boston Children's Hospital.

16S rRNA pyrosequencing and data analysis

Methods describing bacterial rRNA sequencing and analysis are detailed in the Supplemental Information section.

DSS and lymphopenia-induce colitis

DSS-induced colitis was initiated by treating mice with 3.5-5% DSS (MP Biomedicals) in the drinking water ad libitum for 5 days, as indicated (Geuking et al., 2011). The DSS solution was then replaced by normal water for the indicated periods, following which the mice were euthanized. Subgroups of mice were injected *i.p.* with 300 μg of neutralizing IL-17A mouse antibody (17F3) or IgG1 isotype control antibodies(MOPC21) (Bio × Cell) on days 0, 2, and 4 of the DSS protocol. Body weights were monitored daily. Histological

assessments of colitis and severity scores were carried out in a blinded manner after hematoxylin and eosin (H&E) staining.

For Lymphopenia-induced colitis, $Rag1^{-/-}$ mice were injected *i.p.* with 5×10^5 congenic $CD45.1^+CD4^+CD45RB^{high}$ T cells (Haribhai et al., 2009). Some mice were injected *i.p* with 2.5×10^5 $CD45.2^+CD4^+Foxp3^+$ Treg cells either from $Foxp3^{EGPFCre}$ or $Foxp3^{EGFPCre}MyD88^{/}$ mice at the same time. Mice were observed daily and weighed weekly. Mice developed clinical signs of colitis around week 4 post transferred.

Mouse colonization with OVA$_{139-386}$DH5α bacteria

Chicken OVA$_{139-386}$-expressing *E coli* (DH5α *E. coli* strain) was a kind gift of Dr. Rick Blumberg (Beth Israel Deaconess Hospital, Boston) (Yoshida et al., 2006). Control DH5α *E. Coli* bacteria, harboring the parent low-copy plasmid pACYC184 (chloramphenicol selection), was obtained from New England Biolabs. Bacteria were grown under chloramphenicol selection, harvested by centrifugation and orally gavaged at 10^{10} Colon form units (CFU)/ 500μl PBS/per mouse (Hapfelmeier et al., 2010). The mice were then sensitized with OVA ad libitum for 1 week. Stool, lung and liver were isolated from the inoculated mice and analyzed for chloramphenicol-resistant bacteria by plating serial dilutions and counting CFUs.

Adoptive cell transfers

For *in vivo* iTreg cells conversion experiments, naïve OT-II (Vα2$^+$) CD4$^+$Foxp3$^-$(EGFP$^-$) Tconv cells were isolated from spleens of OT-II$^+$ $Foxp3^{EGFPcre}$ or OT-II$^+$ $Foxp3^{EGFPcre}Myd88^{/}$ mice by cell sorting using BD FACSAria III (BD Biosciences) (purity >95%). The cells were labeled with Violet CellTrace Dye (Invitrogen) and adoptively transferred (1×10^6) by retro-orbital injection into congenic *CD45.1* mice. Recipient mice were then administered OVA in drinking water ad libitum for 1 week. The different organs were thereafter collected and analyzed by flow cytometry for Violet CellTrace Dye, Vα2 and EGFP.

Adoptive transfer of splenic Treg cells from $Foxp3^{EGFPcre}$ and $Foxp3^{EGFPcre}Myd88^{/}$ - mice into $Tcra^{-/-}$ mice was carried out as above. Recipient mice were analyzed two weeks later for T and B cell phenotypes and numbers in the PP and other immune tissues.

Adoptive transfer of PP B cells

PP cells of CD45.1 congenic donor mice were isolated and stained with PE-labeled anti-IgA, APC-labeled anti-IgG and PB-labeled anti-B220 IgG mAbs. B220$^+$IgG$^+$ and B220$^+$IgA$^+$ B cells were isolated to 95-98% purity by cell sorting using BD FACSAria III (BD Biosciences). After isolation, 2-5 $\times 10^5$ cells of the indicated cell types were immediately transferred *i.p.* into CD45.2 recipient mice. Two weeks later, the recipient mice were euthanized for analysis.

Statistical analysis

Statistical significance between groups was determined by the unpaired, two-tailed student's *t* test, One-way and two-way ANOVA using Prism software (GraphPad). Statistical analyses

Author Manuscript

of gut bacterial 16S rRNA studies were carried out as detailed in the Supplemental Information section. Differences at P < 0.05 were considered significant. Data are presented either as means or means ± SEM.

Supplementary Material

Refer to Web version on PubMed Central for supplementary material.

REFERENCES

Atarashi K, Tanoue T, Shima T, Imaoka A, Kuwahara T, Momose Y, Cheng G, Yamasaki S, Saito T, Ohba Y, et al. Induction of colonic regulatory T cells by indigenous Clostridium species. Science. 2011; 331:337–341. [PubMed: 21205640]

Backhed F, Ley RE, Sonnenburg JL, Peterson DA, Gordon JI. Host-bacterial mutualism in the human intestine. Science. 2005; 307:1915–1920. [PubMed: 15790844]

Caramalho I, Lopes-Carvalho T, Ostler D, Zelenay S, Haury M, Demengeot J. Regulatory T cells selectively express toll-like receptors and are activated by lipopolysaccharide. J Exp Med. 2003; 197:403–411. [PubMed: 12591899]

Chaudhry A, Rudra D, Treuting P, Samstein RM, Liang Y, Kas A, Rudensky AY. CD4+ regulatory T cells control TH17 responses in a Stat3-dependent manner. Science. 2009; 326:986–991. [PubMed: 19797626]

Chaudhry A, Samstein RM, Treuting P, Liang Y, Pils MC, Heinrich JM, Jack RS, Wunderlich FT, Bruning JC, Muller W, Rudensky AY. Interleukin-10 signaling in regulatory T cells is required for suppression of Th17 cell-mediated inflammation. Immunity. 2011; 34:566–578. [PubMed: 21511185]

Chen Q, Davidson TS, Huter EN, Shevach EM. Engagement of TLR2 does not reverse the suppressor function of mouse regulatory T cells, but promotes their survival. J Immunol. 2009; 183:4458–4466. [PubMed: 19748987]

Chu H, Mazmanian SK. Innate immune recognition of the microbiota promotes host-microbial symbiosis. Nat Immunol. 2013; 14:668–675. [PubMed: 23778794]

Cong Y, Feng T, Fujihashi K, Schoeb TR, Elson CO. A dominant, coordinated T regulatory cell-IgA response to the intestinal microbiota. Proc Natl Acad Sci U S A. 2009; 106:19256–19261. [PubMed: 19889972]

Coombes JL, Siddiqui KR, Arancibia-Carcamo CV, Hall J, Sun CM, Belkaid Y, Powrie F. A functionally specialized population of mucosal CD103+ DCs induces Foxp3+ regulatory T cells via a TGF-beta and retinoic acid-dependent mechanism. J Exp Med. 2007; 204:1757–1764. [PubMed: 17620361]

Fagarasan S, Kawamoto S, Kanagawa O, Suzuki K. Adaptive immune regulation in the gut: T cell-dependent and T cell-independent IgA synthesis. Annu Rev Immunol. 2010; 28:243–273. [PubMed: 20192805]

Gaboriau-Routhiau V, Rakotobe S, Lecuyer E, Mulder I, Lan A, Bridonneau C, Rochet V, Pisi A, De Paepe M, Brandi G, et al. The key role of segmented filamentous bacteria in the coordinated maturation of gut helper T cell responses. Immunity. 2009; 31:677–689. [PubMed: 19833089]

Geuking MB, Cahenzli J, Lawson MA, Ng DC, Slack E, Hapfelmeier S, McCoy KD, Macpherson AJ. Intestinal bacterial colonization induces mutualistic regulatory T cell responses. Immunity. 2011; 34:794–806. [PubMed: 21596591]

Hapfelmeier S, Lawson MA, Slack E, Kirundi JK, Stoel M, Heikenwalder M, Cahenzli J, Velykoredko Y, Balmer ML, Endt K, et al. Reversible microbial colonization of germ-free mice reveals the dynamics of IgA immune responses. Science. 2010; 328:1705–1709. [PubMed: 20576892]

Haribhai D, Lin W, Edwards B, Ziegelbauer J, Salzman NH, Carlson MR, Li SH, Simpson PM, Chatila TA, Williams CB. A central role for induced regulatory T cells in tolerance induction in experimental colitis. J Immunol. 2009; 182:3461–3468. [PubMed: 19265124]

Haribhai D, Lin W, Relland LM, Truong N, Williams CB, Chatila TA. Regulatory T cells dynamically control the primary immune response to foreign antigen. J Immunol. 2007; 178:2961–2972. [PubMed: 17312141]

Haribhai D, Williams JB, Jia S, Nickerson D, Schmitt EG, Edwards B, Ziegelbauer J, Yassai M, Li SH, Relland LM, et al. A requisite role for induced regulatory T cells in tolerance based on expanding antigen receptor diversity. Immunity. 2011; 35:109–122. [PubMed: 21723159]

Hirota K, Turner JE, Villa M, Duarte JH, Demengeot J, Steinmetz OM, Stockinger B. Plasticity of Th17 cells in Peyer's patches is responsible for the induction of T cell-dependent IgA responses. Nat Immunol. 2013; 14:372–379. [PubMed: 23475182]

Hooper LV, Littman DR, Macpherson AJ. Interactions between the microbiota and the immune system. Science. 2012; 336:1268–1273. [PubMed: 22674334]

Hou B, Benson A, Kuzmich L, DeFranco AL, Yarovinsky F. Critical coordination of innate immune defense against Toxoplasma gondii by dendritic cells responding via their Toll-like receptors. Proc Natl Acad Sci U S A. 2011; 108:278–283. [PubMed: 21173242]

Hsieh CS, Liang Y, Tyznik AJ, Self SG, Liggitt D, Rudensky AY. Recognition of the peripheral self by naturally arising CD25+ CD4+ T cell receptors. Immunity. 2004; 21:267–277. [PubMed: 15308106]

Ivanov II, Atarashi K, Manel N, Brodie EL, Shima T, Karaoz U, Wei D, Goldfarb KC, Santee CA, Lynch SV, et al. Induction of intestinal Th17 cells by segmented filamentous bacteria. Cell. 2009; 139:485–498. [PubMed: 19836068]

Izcue A, Coombes JL, Powrie F. Regulatory lymphocytes and intestinal inflammation. Annu Rev Immunol. 2009; 27:313–338. [PubMed: 19302043]

Jabara HH, McDonald DR, Janssen E, Massaad MJ, Ramesh N, Borzutzky A, Rauter I, Benson H, Schneider L, Baxi S, et al. DOCK8 functions as an adaptor that links TLR-MyD88 signaling to B cell activation. Nat Immunol. 2012; 13:612–620. [PubMed: 22581261]

Josefowicz SZ, Lu LF, Rudensky AY. Regulatory T cells: mechanisms of differentiation and function. Annu Rev Immunol. 2012; 30:531–564. [PubMed: 22224781]

Kawai T, Akira S. Signaling to NF-kappaB by Toll-like receptors. Trends Mol Med. 2007; 13:460–469. [PubMed: 18029230]

Kawamoto S, Maruya M, Kato LM, Suda W, Atarashi K, Doi Y, Tsutsui Y, Qin H, Honda K, Okada T, et al. Foxp3(+) T cells regulate immunoglobulin a selection and facilitate diversification of bacterial species responsible for immune homeostasis. Immunity. 2014; 41:152–165. [PubMed: 25017466]

Lathrop SK, Bloom SM, Rao SM, Nutsch K, Lio CW, Santacruz N, Peterson DA, Stappenbeck TS, Hsieh CS. Peripheral education of the immune system by colonic commensal microbiota. Nature. 2011

Lathrop SK, Santacruz NA, Pham D, Luo J, Hsieh CS. Antigen-specific peripheral shaping of the natural regulatory T cell population. J Exp Med. 2008; 205:3105–3117. [PubMed: 19064700]

Laurence A, Amarnath S, Mariotti J, Kim YC, Foley J, Eckhaus M, O'Shea JJ, Fowler DH. STAT3 transcription factor promotes instability of nTreg cells and limits generation of iTreg cells during acute murine graft-versus-host disease. Immunity. 2012; 37:209–222. [PubMed: 22921119]

Lecuyer E, Rakotobe S, Lengline-Garnier H, Lebreton C, Picard M, Juste C, Fritzen R, Eberl G, McCoy KD, Macpherson AJ, et al. Segmented filamentous bacterium uses secondary and tertiary lymphoid tissues to induce gut IgA and specific T helper 17 cell responses. Immunity. 2014; 40:608–620. [PubMed: 24745335]

Lee YK, Mazmanian SK. Has the microbiota played a critical role in the evolution of the adaptive immune system? Science. 2010; 330:1768–1773. [PubMed: 21205662]

Liu H, Komai-Koma M, Xu D, Liew FY. Toll-like receptor 2 signaling modulates the functions of CD4+ CD25+ regulatory T cells. Proc Natl Acad Sci U S A. 2006; 103:7048–7053. [PubMed: 16632602]

Long M, Park SG, Strickland I, Hayden MS, Ghosh S. Nuclear factor-kappaB modulates regulatory T cell development by directly regulating expression of Foxp3 transcription factor. Immunity. 2009; 31:921–931. [PubMed: 20064449]

Ma CS, Avery DT, Chan A, Batten M, Bustamante J, Boisson-Dupuis S, Arkwright PD, Kreins AY, Averbuch D, Engelhard D, et al. Functional STAT3 deficiency compromises the generation of human T follicular helper cells. Blood. 2012; 119:3997–4008. [PubMed: 22403255]

Mucida D, Kutchukhidze N, Erazo A, Russo M, Lafaille JJ, Curotto de Lafaille MA. Oral tolerance in the absence of naturally occurring Tregs. J Clin Invest. 2005; 115:1923–1933. [PubMed: 15937545]

Mucida D, Park Y, Kim G, Turovskaya O, Scott I, Kronenberg M, Cheroutre H. Reciprocal TH17 and regulatory T cell differentiation mediated by retinoic acid. Science. 2007; 317:256–260. [PubMed: 17569825]

Murtaugh LC, Stanger BZ, Kwan KM, Melton DA. Notch signaling controls multiple steps of pancreatic differentiation. Proc Natl Acad Sci U S A. 2003; 100:14920–14925. [PubMed: 14657333]

Nutsch KM, Hsieh CS. T cell tolerance and immunity to commensal bacteria. Current opinion in immunology. 2012; 24:385–391. [PubMed: 22613090]

Palm NW, de Zoete MR, Cullen TW, Barry NA, Stefanowski J, Hao L, Degnan PH, Hu J, Peter I, Zhang W, et al. Immunoglobulin a coating identifies colitogenic bacteria in inflammatory bowel disease. Cell. 2014; 158:1000–1010. [PubMed: 25171403]

Palm NW, Medzhitov R. Pattern recognition receptors and control of adaptive immunity. Immunol Rev. 2009; 227:221–233. [PubMed: 19120487]

Peterson DA, McNulty NP, Guruge JL, Gordon JI. IgA response to symbiotic bacteria as a mediator of gut homeostasis. Cell Host Microbe. 2007; 2:328–339. [PubMed: 18005754]

Rivas MN, Koh YT, Chen A, Nguyen A, Lee YH, Lawson G, Chatila TA. MyD88 is critically involved in immune tolerance breakdown at environmental interfaces of Foxp3-deficient mice. J Clin Invest. 2012; 122:1933–1947. [PubMed: 22466646]

Round JL, Lee SM, Li J, Tran G, Jabri B, Chatila TA, Mazmanian SK. The Toll-like receptor 2 pathway establishes colonization by a commensal of the human microbiota. Science. 2011; 332:974–977. [PubMed: 21512004]

Round JL, Mazmanian SK. The gut microbiota shapes intestinal immune responses during health and disease. Nat Rev Immunol. 2009; 9:313–323. [PubMed: 19343057]

Round JL, Mazmanian SK. Inducible Foxp3+ regulatory T-cell development by a commensal bacterium of the intestinal microbiota. Proc Natl Acad Sci U S A. 2010; 107:12204–12209. [PubMed: 20566854]

Rubtsov YP, Rasmussen JP, Chi EY, Fontenot J, Castelli L, Ye X, Treuting P, Siewe L, Roers A, Henderson WR Jr. et al. Regulatory T cell-derived interleukin-10 limits inflammation at environmental interfaces. Immunity. 2008; 28:546–558. [PubMed: 18387831]

Sasaki Y, Derudder E, Hobeika E, Pelanda R, Reth M, Rajewsky K, Schmidt-Supprian M. Canonical NF-kappaB activity, dispensable for B cell development, replaces BAFF-receptor signals and promotes B cell proliferation upon activation. Immunity. 2006; 24:729–739. [PubMed: 16782029]

Sun CM, Hall JA, Blank RB, Bouladoux N, Oukka M, Mora JR, Belkaid Y. Small intestine lamina propria dendritic cells promote de novo generation of Foxp3 T reg cells via retinoic acid. J Exp Med. 2007; 204:1775–1785. [PubMed: 17620362]

Sutmuller RP, den Brok MH, Kramer M, Bennink EJ, Toonen LW, Kullberg BJ, Joosten LA, Akira S, Netea MG, Adema GJ. Toll-like receptor 2 controls expansion and function of regulatory T cells. J Clin Invest. 2006; 116:485–494. [PubMed: 16424940]

Suzuki K, Meek B, Doi Y, Muramatsu M, Chiba T, Honjo T, Fagarasan S. Aberrant expansion of segmented filamentous bacteria in IgA-deficient gut. Proc Natl Acad Sci U S A. 2004; 101:1981–1986. [PubMed: 14766966]

Tsuji M, Komatsu N, Kawamoto S, Suzuki K, Kanagawa O, Honjo T, Hori S, Fagarasan S. Preferential generation of follicular B helper T cells from Foxp3+ T cells in gut Peyer's patches. Science. 2009; 323:1488–1492. [PubMed: 19286559]

Wang Q, McLoughlin RM, Cobb BA, Charrel-Dennis M, Zaleski KJ, Golenbock D, Tzianabos AO, Kasper DL. A bacterial carbohydrate links innate and adaptive responses through Toll-like receptor 2. J Exp Med. 2006; 203:2853–2863. [PubMed: 17178920]

Wang Y, Su MA, Wan YY. An essential role of the transcription factor GATA-3 for the function of regulatory T cells. Immunity. 2011; 35:337–348. [PubMed: 21924928]

Wohlfert EA, Grainger JR, Bouladoux N, Konkel JE, Oldenhove G, Ribeiro CH, Hall JA, Yagi R, Naik S, Bhairavabhotla R, et al. GATA3 controls Foxp3(+) regulatory T cell fate during inflammation in mice. J Clin Invest. 2011; 121:4503–4515. [PubMed: 21965331]

Yang X, Klein R, Tian X, Cheng HT, Kopan R, Shen J. Notch activation induces apoptosis in neural progenitor cells through a p53-dependent pathway. Dev Biol. 2004; 269:81–94. [PubMed: 15081359]

Yoshida M, Kobayashi K, Kuo TT, Bry L, Glickman JN, Claypool SM, Kaser A, Nagaishi T, Higgins DE, Mizoguchi E, et al. Neonatal Fc receptor for IgG regulates mucosal immune responses to luminal bacteria. J Clin Invest. 2006; 116:2142–2151. [PubMed: 16841095]

Zhou X, Bailey-Bucktrout SL, Jeker LT, Penaranda C, Martinez-Llordella M, Ashby M, Nakayama M, Rosenthal W, Bluestone JA. Instability of the transcription factor Foxp3 leads to the generation of pathogenic memory T cells in vivo. Nat Immunol. 2009; 10:1000–1007. [PubMed: 19633673]
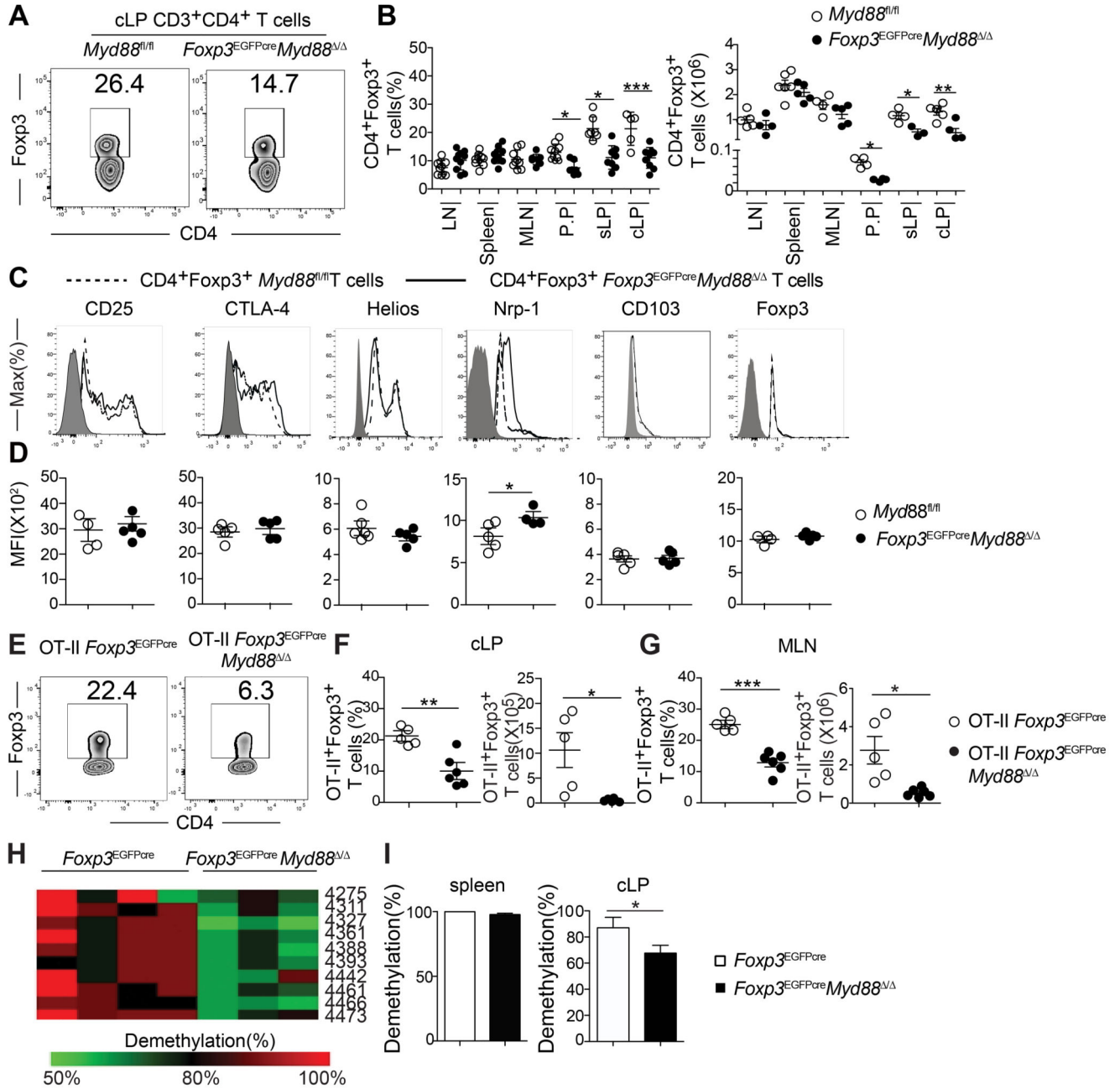
Figure 1. Treg cell-specific MyD88 deletion results in gut mucosa Treg cell deficiency
A. Flow cytometric analysis of CD4$^+$Foxp3$^+$ Treg cells in the cLP of *Myd88$^{fl/fl}$* and
Foxp3^{EGFPcre}Myd88$^{Δ/Δ}$ mice. **B**. Frequencies and absolute numbers of Treg cells in
different tissues of *Myd88$^{fl/fl}$* and *Foxp3^{EGFPcre}Myd88$^{Δ/Δ}$* mice. **C, D**. Flow cytometric
analysis (**C**) and mean fluorescence intensity (MFI) (**D**) of CD25, CTLA-4, Helios, Nrp1,
CD103 and Foxp3 cLP Treg cells of *Myd88$^{fl/fl}$* and *Foxp3^{EGFPcre}Myd88$^{Δ/Δ}$* mice. **E.** Flow
cytometric analysis of Foxp3 expression in cLP CD45.2$^+$CD4$^+$ T cells in CD45.1$^+$ WT mice
that received naïve CD45.2$^+$CD4$^+$Foxp3$^-$ T cells from OT-II$^+$ *Foxp3^{EGFPcre}* or OT-II$^+$
Foxp3^{EGFPcre}Myd88$^{Δ/Δ}$ mice and were then fed OVA in the drinking water for 1 week. **F.**

Frequencies (left panel) and absolute numbers (right panel) of donor CD45.2$^+$CD4$^+$EGFP$^+$ iTreg in the cLP of recipient mice from panel (**E**). **G**. Absolute numbers of donor CD45.2$^+$CD4$^+$Foxp3^{EGFP+} iTreg in the MLN of recipient mice. **H**. Methylation status of individual CpG motifs within the *Foxp3* CNS2 in cLP Treg cells of *Foxp3^{EGFPcre}* and *Foxp3^{EGFPcre}Myd88$^{-/-}$* mice. Individual CpG motifs are numbered with reference to the transcription initiation site of *Foxp3*. **I**. Global methylation status of Foxp3 CNS2 in splenic and cLP Treg cells shown in **H**. Results are representative of 4 independent experiments. N=3-8 mice/group. *p<0.05; **p<0.01; ***p<0.001 by Student's unpaired two tailed *t* test and One-way ANOVA.
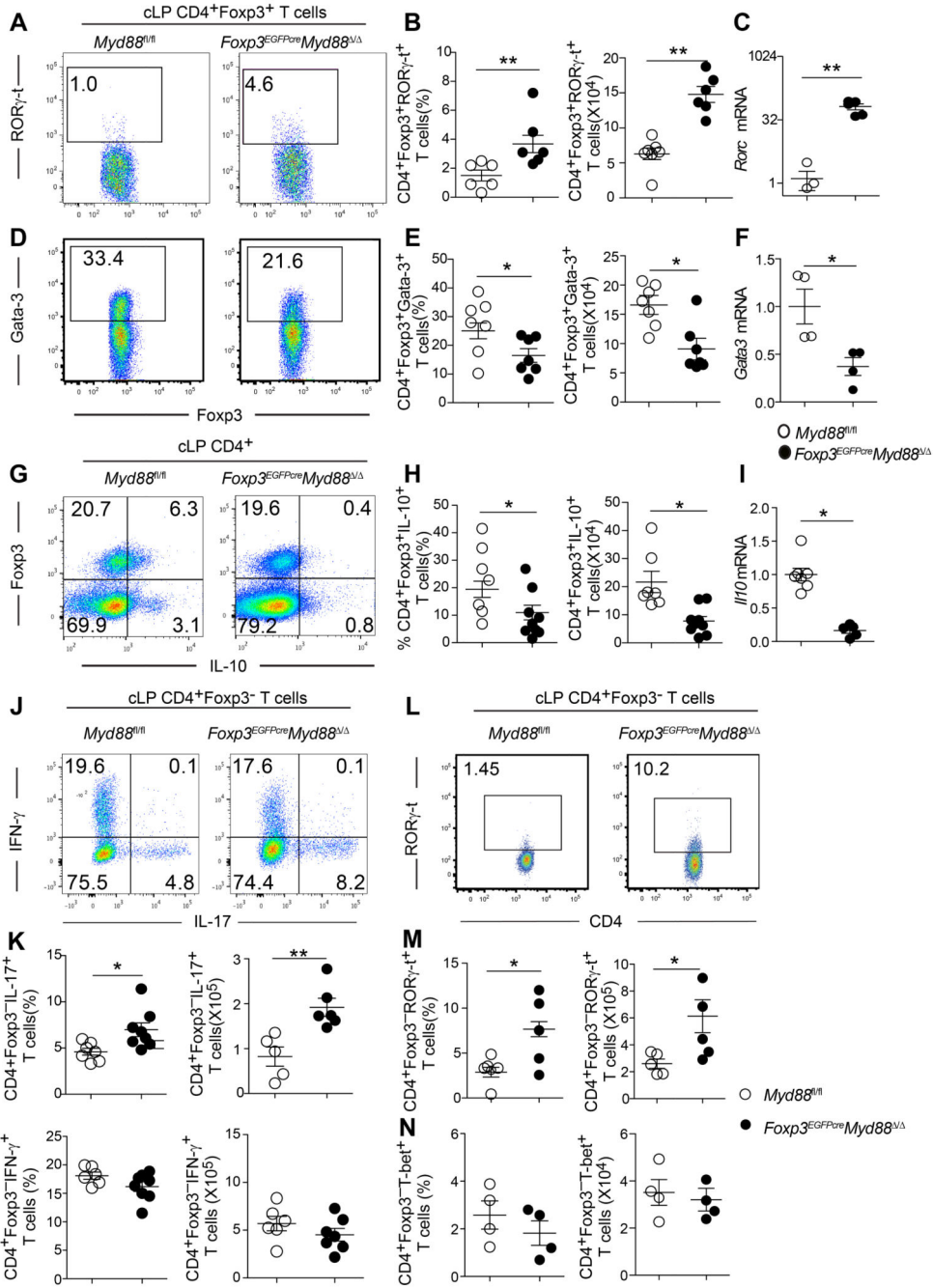
Figure 2. Treg cell-specific MyD88 deletion results in colonic Th17 skewing

A, B. Flow cytometric analysis (**A**) and enumerated cell frequencies and numbers (**B**) of cLP RORγ-t⁺CD4⁺Foxp3⁺Treg cells in *Myd88^fl/fl* and *Foxp3^EGFPcre^Myd88^Δ/Δ* mice. **C.** Real time PCR analysis of *Rorc* expression in cell-sorted cLP CD4⁺Foxp3⁺ Treg cells. **D-I**. Analysis of GATA3 expression and *Gata3* mRNA (**D-F**) and IL-10 expression and *Il10* mRNA (**G-I**) in cLP CD4⁺Foxp3⁺ Treg cells of the respective mouse strain, performed as in **A-C**. **J, K.** Expression of IL-17 and IFN-γ in cLP CD4⁺Foxp3⁻ T cells of *Myd88^fl/fl* and *Foxp3^EGFPcre^Myd88^Δ/Δ* mice. Flow cytometric analysis (**J**), frequencies and absolute

numbers (**K**) of cytokine expressing cells. **L, M.** Flow cytometric analysis (**L**), and frequencies and absolute numbers (**M**) of cLP CD4$^+$Foxp3$^-$RORγ-t$^+$ T cells of the respective mouse strain. **N**. Frequencies (left panel) and total cell number (right panel) of cLP CD4$^+$Foxp3$^-$T-bet$^+$ of *Foxp3^{EGFPcre}Myd88$^{/}$* mice compared with *Myd88$^{fl/fl}$* control mice. Results are representative of 4 independent experiments. N=4-7 mice/group. *p<0.05; **p<0.01; ***p<0.001 by Student's unpaired two tailed *t* test.
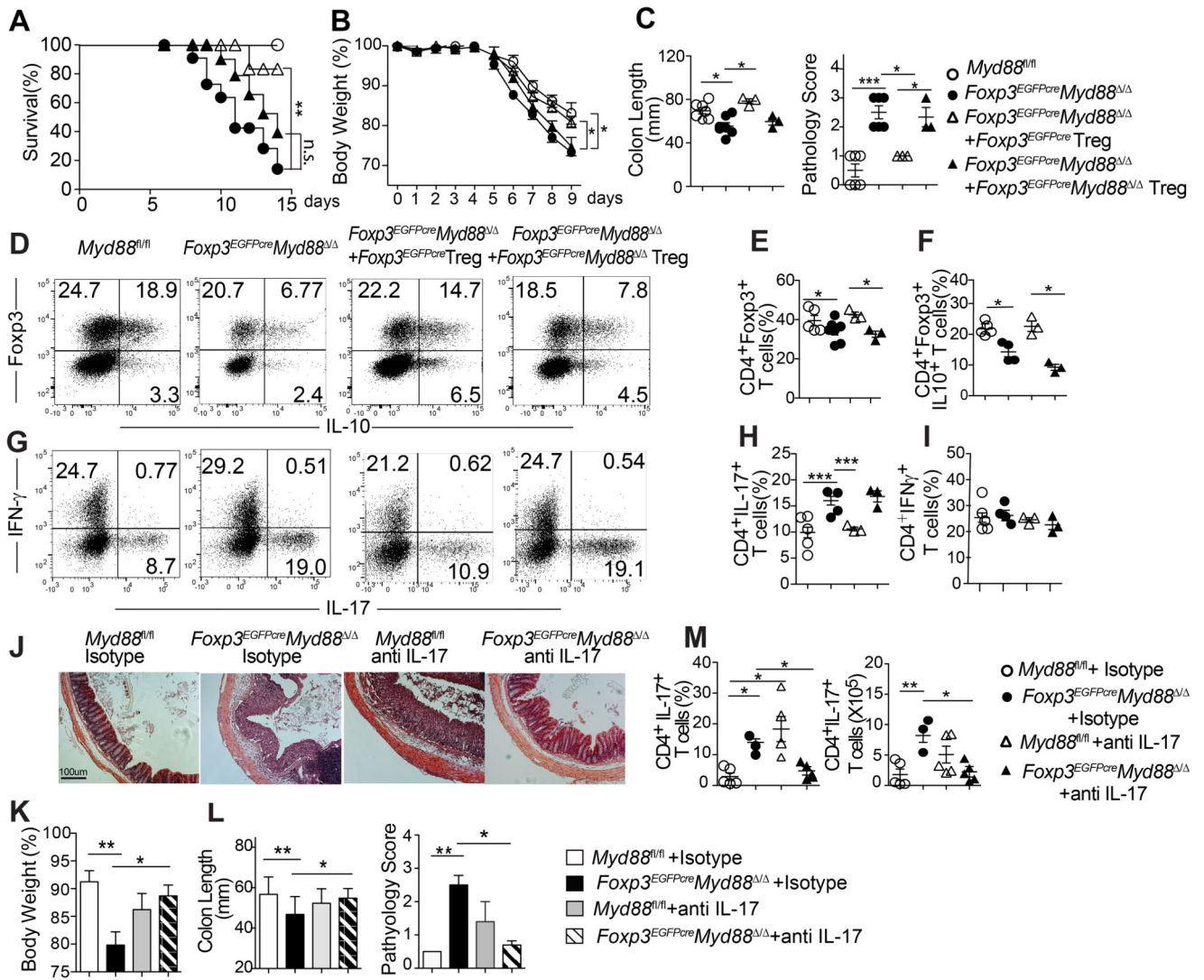
Figure 3. Treg cell-specific MyD88 deficiency aggravates the severity of experimental colitis
A. Survival curves of the following mouse groups treated with 5% DSS for 5 days then followed thereafter: 1) $Myd88^{fl/fl}$, 2) $Foxp3^{EGFPcre}Myd88^{\Delta/\Delta}$ and 3, 4) $Foxp3^{EGFPcre}Myd88^{\Delta/\Delta}$ mice that were given cell-sorted CD4$^+$EGFP$^+$ splenic Treg cells from either $Foxp3^{EGFPcre}$ (MyD88-sufficient) or $Foxp3^{EGFPcre}Myd88^{\Delta/\Delta}$ (MyD88-defcient) mice. **B.** Body weight loss following treatment of mouse groups as in panel **A** with 3.5% DSS for 5 days. **C**. Colon length and histological scores of the respective mouse groups in (**B**) at day 9 post DSS treatment. **D-I.** Flow cytometric analysis and frequencies of total and IL-10$^+$ CD4$^+$Foxp3$^+$ Treg cells (D-F) and IFN-γ and IL-17 secreting CD4$^+$Foxp3$^-$ Tconv cells (**G-I**) isolated from the cLP of the respective mouse groups in (**B, C**) at day 9 post DSS treatment. **J-M.** Groups of $Foxp3^{EGFPcre}$ and $Foxp3^{EGFPcre}Myd88^{\Delta/\Delta}$ mice were subjected to DSS-induced colitis and treated with either isotype control or neutralizing anti-IL-17A mAbs at days 0, 2, and 4 of DSS treatment. **J**. Colon histology (Hematoxylin and eosin staining; 40× magnification). Body weight loss (**K**), colon length and clinical score (**L**) of the respective mouse groups. **M**. Frequencies and absolute numbers of IL-17 and IFN-γ
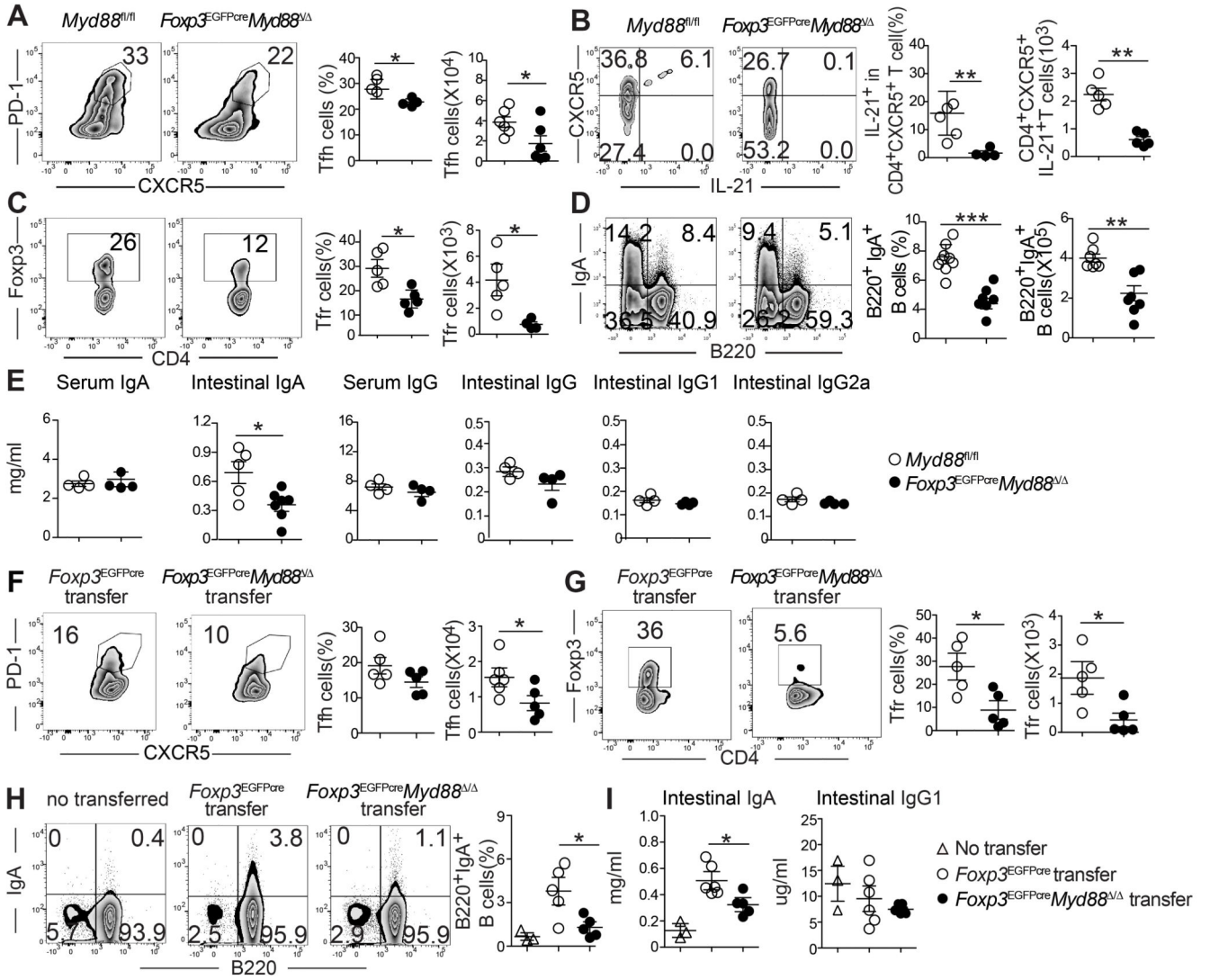
secreting cLP CD4$^+$Foxp3$^-$ Tconv cells of the respective mouse groups. Results are representative of 3 independent experiments. N =9-10 mice/group for panel A; **p<0.01 by log rank test. N= 4-7 mice/group for panels B-M; *p<0.05; **p<0.01; ***p<0.001 by One-way ANOVA.
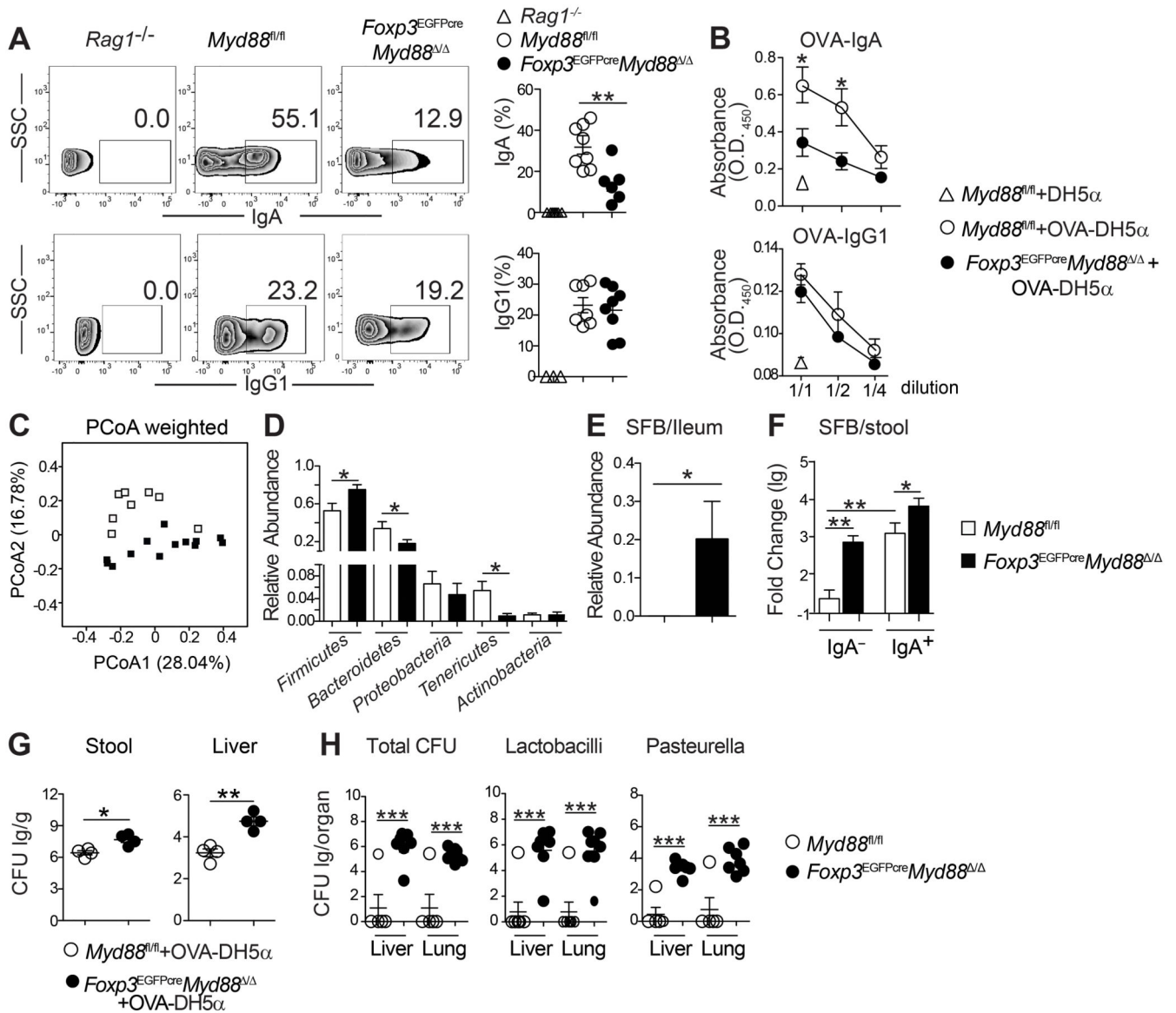
Figure 4. Treg cell-specific MyD88 deficiency impairs PP Tfr and Tfh cell differentiation and intestinal IgA production

A-D. Flow cytometric analysis, frequencies and absolute numbers of Tfh cells (CD4$^+$CXCR5$^+$PD-1^{high}) (**A**), CXCR5$^+$IL-21$^+$ cells within the Tfh populations (**B**), Tfr cells (CD4$^+$Foxp3$^+$CXCR5$^+$PD-1^{high}) (**C**) and IgA$^+$B220$^+$ B cells (**D**) in PP of *Foxp3^{EGFPcre}Myd88$^{Δ/Δ}$* and *Myd88$^{fl/fl}$* mice. **E**. Serum and intestinal lavage fluid concentrations of IgA (**I**) and IgG, IgG1 and IgG2a (**J**) in *Foxp3^{EGFPcre}Myd88$^{Δ/Δ}$* and *Myd88$^{fl/fl}$* mice. **F-H.** Flow cytometric analysis, and frequencies and absolute numbers of Tfh (**F**), Tfr (**G**) and IgA$^+$B220$^+$ (**H**) cells isolated from the PP of *Tcra$^{-/-}$* mice 2 weeks following the transfer of CD4$^+$EGFP$^+$Treg cells isolated from either *Foxp3^{EGFPcre}* or *Foxp3^{EGFPcre}Myd88$^{Δ/Δ}$*. **I.** Luminal concentration of IgA and IgG1 in the mouse groups from panel (**H**). Results are representative of 3 independent experiments. N=3-5 mice/group. *p<0.05; **p<0.01; by Student's unpaired two tailed *t* test.

Figure 5. T$_R$-cell specific MyD88 deficiency promotes dysbiosis and and bacterial translocation to deep tissues

A. Flow cytometric analysis and frequencies of IgA- and IgG1-coated bacteria in the fecal pellets of *Rag1$^{-/-}$*, *Foxp3^{EGFPcre}Myd88$^{Δ/Δ}$* and *MyD88$^{fl/fl}$* mice. **B.** OVA-specific luminal IgA and IgG1 concentrations in mice (panel A) gavaged with OVA-DH5α bacteria. **C.** Weighted Unifrac plot of ileal mucosa-associated microbial communities, visualized with principal coordinate analysis (PCoA), in *Foxp3^{EGFPcre}Myd88$^{Δ/Δ}$* versus *Myd88$^{fl/fl}$* mice (*p*-value = 0.001 by AMOVA). **D**. Relative abundance of different microbial phyla in ileal mucosa-associated microbiota in *Foxp3^{EGFPcre}Myd88$^{Δ/Δ}$* and *Myd88$^{fl/fl}$* mice (*false discovery rate<0.05)**. E.** Relative abundance of SFB taxa in illeal mucosa-associated microbiota in *Foxp3^{EGFPcre}Myd88$^{Δ/Δ}$* and *Myd88$^{fl/fl}$* mice. **F.** Real time PCR analysis of SFB 16S rRNA in IgA$^+$ and IgA$^-$ fecal bacterial fractions of *Myd88$^{fl/fl}$* and *Foxp3^{EGFPcre}Myd88$^{Δ/Δ}$* mice. **G**. Stool (left panel) and liver (right panel) OVA-DH5α
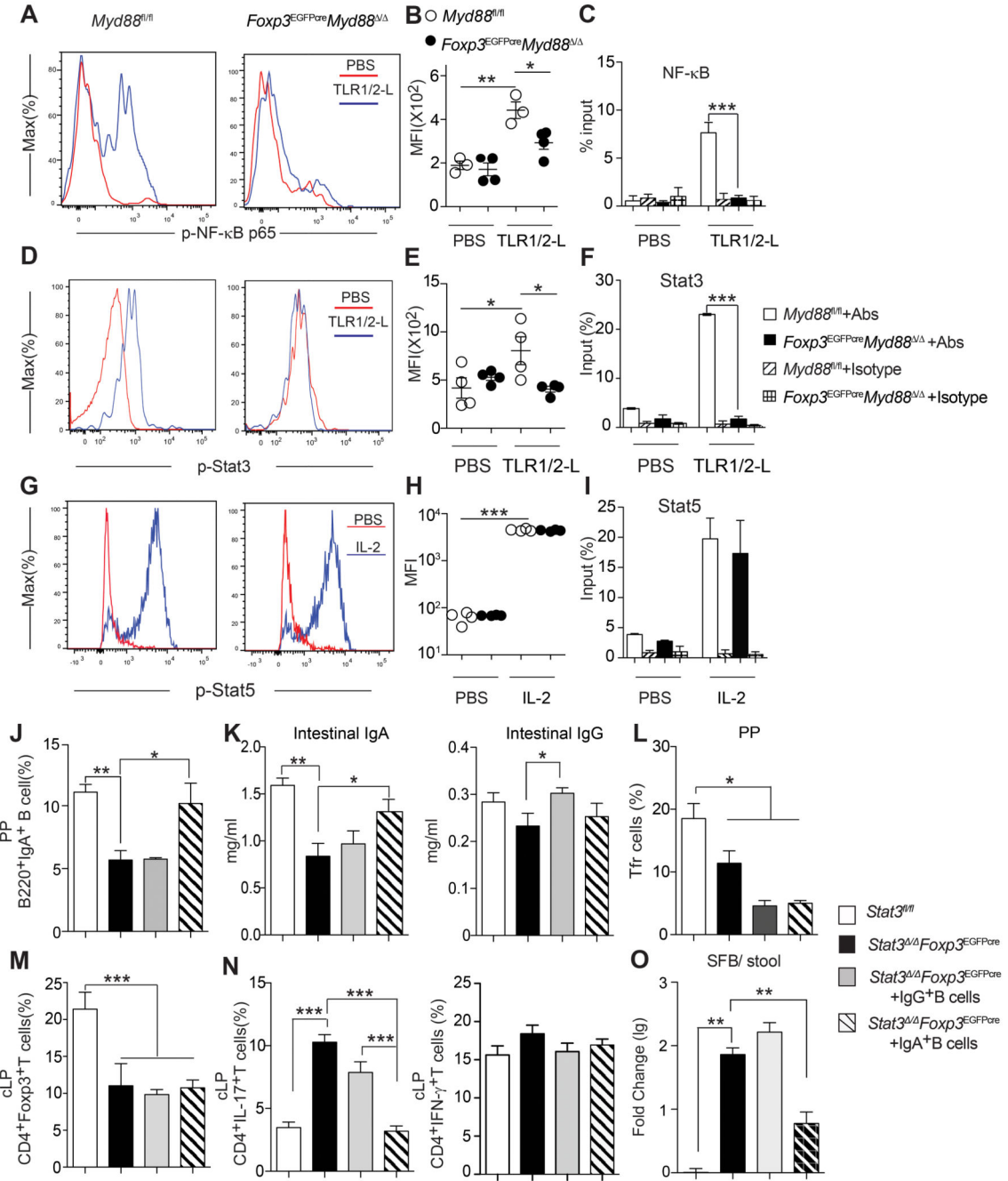
bacterial load [expressed as log colony forming units (lg CFU)/g] in $Foxp3^{EGFPcre}Myd88^{/}$ and $Myd88^{fl/fl}$ mice treated with the OVA-DH5α bacteria by oral gavage. **H**. Loads of total bacteria, *Lactobacilli* and *Pasteurella* (all expressed as CFU/g tissue) in the lung and liver of $Myd88^{fl/fl}$ and $Foxp3^{EGFPcre}Myd88^{/}$ mice. Results are representative of 3 independent experiments. Results representative of 3 independent experiments. N=5 mice/group. *p<0.05; **p<0.01; by Student's unpaired two tailed *t* test.
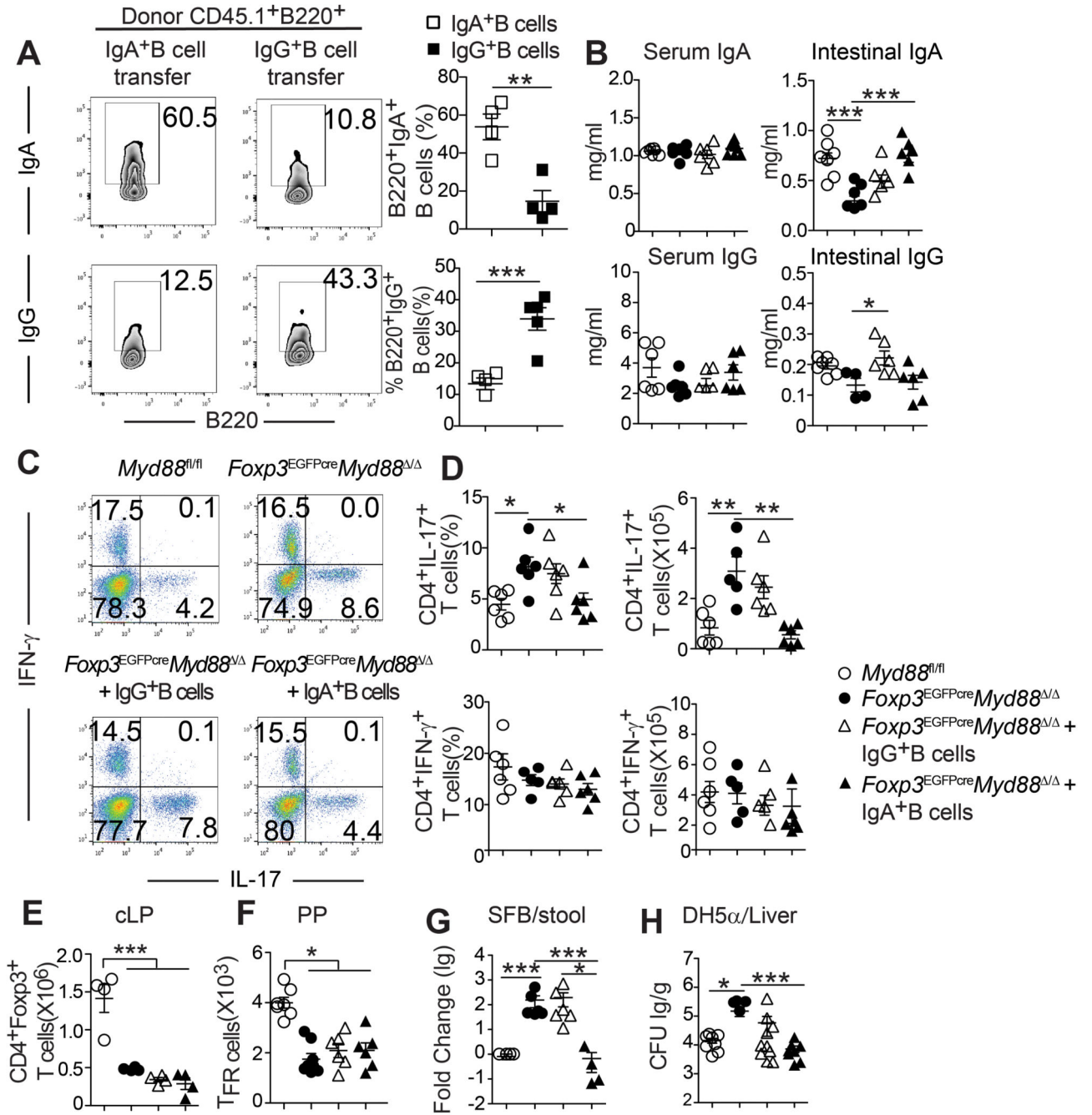
Figure 6. Adoptive transfer of IgA$^+$ PP B cells restores intestinal IgA production and inhibits Th17 skewing in $Foxp3^{EGFPcre}Myd88^{\Delta/\Delta}$ recipients

A. Flow cytometric analysis and frequencies of CD45.1$^+$B220$^+$IgA$^+$ and CD45.1$^+$B220$^+$IgG$^+$ B cells found in the PP of $Myd88^{fl/fl}$ and $Foxp3^{EGFPcre}Myd88^{\Delta/\Delta}$ recipients 2 weeks following their adoptive transfer. **B.** Serum and intestinal IgA (upper panels) and IgG1 (lower panels) concentrations in sham treated $Myd88^{fl/fl}$ and $Foxp3^{EGFPcre}Myd88^{\Delta/\Delta}$ mice and in $Foxp3^{EGFPcre}Myd88^{\Delta/\Delta}$ mice that received CD45.1$^+$B220$^+$IgA$^+$ and CD45.1$^+$B220$^+$IgG$^+$ B cells. **C, D.** Flow cytometric analysis (**C**),

frequencies and absolute numbers (**D**) of IL-17 and IFN-γ -expressing cLP CD4$^+$Foxp3$^-$ Tconv cells in the mouse groups described in (**B**). **E, F.** Absolute numbers of Treg cells in the cLP (**E**) and Tfr cells in the PP (**F**) in mouse groups outlined in (**B**). **G.** Real time PCR analysis of SFB 16S rRNA in the fecal pellets of the respective mouse groups**. H**. Translocation of gavaged DH5α bacteria into livers of mice of the respective mouse groups. Results representative of 3 independent experiments. N=3-5 mice/group. *p<0.05; **p<0.01; ***p<0.001 by Student's unpaired two tailed *t* test and one-way ANOVA.

Figure 7. Treg cell-specific MyD88 signaling activates Stat3 and its deficiency is phenocopied by T_R-cell specific Stat3 deficiency

A-I. TLR1-2-mediated activation of p65-NF-κB, Stat3 and Stat5 in *Myd88^{fl/fl}* and *Foxp3^{EGFPcre}Myd88^{Δ/Δ}* cLP CD4^+Foxp3^+Treg cells. **A, D, G**. Flow cytometric analysis of p-p65-NF-κB (**A**), pStat3 (**D**) and pStat5 (**G**) in cLP CD4^+Foxp3^+Treg cells treated with either PBS or the TLR1-2 ligand (TLR1-2-L) Pam3SCK4. (**B, E, H**) MFI of the respective phosphoprotein. (**C, F, I**). Chromatin immunoprecipitation (ChIP) assay of NF-κB p65, Stat3 and Stat5 bound to the Foxp3-CNS2 in the respective cLP CD4^+Foxp3^+Treg cells

treated with either PBS, TLR1-2-L (for p65-NF-kB and Stat3 ChIP) or IL-2 (for Stat5 ChIP). **J-O**. WT and $Foxp3^{EGFPcre}Stat3^{/}$ mice were either untreated or received adoptively transferred CD45.1$^+$B220$^+$IgA$^+$ or CD45.1$^+$B220$^+$IgG$^+$ PP B cell derived from CD45.1$^+$ WT donor mice. Analysis was carried out 2 weeks following the B cell transfer. **J**. Frequencies of total B220$^+$IgA$^+$ in the PP. **K**. Intestinal lavage fluid IgA and IgG concentrations. **L, M**. Frequencies of PP Tfr and cLP Treg cells, respectively. **N**. Frequencies of CD4$^+$IL-17$^+$ and CD4$^+$IFN-γ$^+$ T$_{conv}$ cells. **O**. Real time PCR analysis of SFB 16S rDNA in the stool. Similar results were obtained in 2 independent experiments. N= 4-7 /group *P<0.05; **P<0.01, ***P<0.001 by One-way ANOVA.